JPET Fast Forward. Published on July 20, 2006 as DOI: 10.1124/jpet.106.105858

JPET # 105858

ENZYME- MEDIATED PROTEIN HAPTENATION OF DAPSONE AND SULFAMETHOXAZOLE IN HUMAN KERATINOCYTES – 1. EXPRESSION AND ROLE OF CYTOCHROMES P450

Piyush M. Vyas, Sanjoy Roychowdhury, Farah D. Khan, Thomas E. Prisinzano, Jatinder Lamba, Erin G. Schuetz, Joyce Blaisdell, Joyce A. Goldstein, Kimber L. Munson, Ronald N. Hines, Craig K. Svensson.

Division of Pharmaceutics (SR, PMV, FDK, CKS), Division of Medicinal & Natural Products Chemistry (TP), College of Pharmacy, The University of Iowa, Iowa City, IA; Department of Pharmaceutical Sciences (JL, EGS), St. Jude Children's Hospital, Memphis, TN; Laboratory of Pharmacology & Chemistry (JB, JAG), National Institute of Environmental Health Sciences, Research Triangle Park, NC; Department of Pediatrics and Pharmacology & Toxicology, Medical College of Wisconsin and Children's Research Institute, Children's Hospital of Wisconsin, Milwaukee, WI (KLM, RNH),.

Running Title: Protein haptenation of dapsone and sulfamethoxazole.

Corresponding Author:

Craig K. Svensson, Pharm.D., Ph.D.; Division of Pharmaceutics, College of Pharmacy, The University of Iowa, 115 S. Grand Avenue, S213 PHAR, Iowa City, IA 52242

Tel: (319) 335-8823; Fax: (319) 335-9349; Email: craig-svensson@uiowa.edu

Number of pages of text: 33

Tables: 0

Figures: 9

Number of references: 35

Number of words in abstract: 227

Words in introduction: 501

Words in discussion: 1228

Abbreviations: AA – ascorbic acid; ABT – 1-aminobenzotriazole; CDR – cutaneous drug reactions; COX- cyclooxygenase; CYP450 – cytochromes P450; DDS – dapsone; DDS-NOH – dapsone hydroxylamine; DMAP – 4-dimethylaminopyridine; INDO – indomethacin; MADDS – monoacetyl dapsone; NASMX – N-acetyl sulfamethoxazole; NHEK – normal human epidermal keratinocytes; SMX – sulfamethoxazole; SMX-NOH – sulfamethoxazole hydroxylamine.

Recommended section assignment: Cellular and molecular

ABSTRACT

Cutaneous drug reactions (CDR) are among the most common adverse drug reactions and are responsible for numerous minor to life-threatening complications. Several arylamine drugs, such as sulfamethoxazole (SMX) and dapsone (DDS), undergo bioactivation resulting in adduction to cellular proteins. These adducted proteins may initiate the immune response that ultimately results in a CDR. Recent studies have demonstrated that normal human epidermal keratinocytes (NHEK) can bioactivate these drugs, resulting in protein haptenation. We sought to identify the enzyme(s) responsible for this bioactivation in NHEK. Using immunofluorescence confocal microscopy and an adduct-specific ELISA assay, we found that N-acetylation of the primary amine of SMX and DDS markedly reduced the level of protein haptenation in NHEK. Detection of mRNA and/or protein confirmed the presence of CYP3A4, CYP3A5 and CYP2E1 in NHEK. In contrast, while a faint band suggestive of CYP2C9 protein was detected in one NHEK sample, CYP2C9 message was not detectable. We also examined the ability of chemical inhibitors of cytochromes P450 (aminobenzotriazole and 1-dichloroethylene) and cyclooxygenase (indomethacin) to reduce protein haptenation when NHEK were incubated with SMX or DDS by either confocal microscopy or ELISA. These inhibitors did not significantly attenuate protein adduction with either SMX or DDS, indicating that cytochromes P450 and cyclooxygenase do not play important roles in the bioactivation of these xenobiotics in NHEK and thus suggesting the importance of other enzymes in these cells.

INTRODUCTION

Sulfonamides are used in the treatment of numerous infectious diseases. Their effectiveness in the treatment of *Pneumocystis carinii* pneumonia (PCP), especially in AIDS patients, has increased their importance as therapeutic agents in the modern antimicrobial era (Cribb et al., 1996a). Sulfamethoxazole (SMX) and the sulfone dapsone (DDS) are widely used antimicrobials for the treatment of PCP resulting in the recovery of approximately 75% of the patients suffering from this ailment (Hughes, 1987; Goldie et al., 2002). However, adverse drug reactions, especially those of a cutaneous nature, limit their use. These reactions most commonly occur 7-10 days after initiation of therapy and are associated with fever and skin rash. Morbilliform or maculopapular, non-urticarial types of skin rash are most commonly observed with these agents. Some patients, however, progress to Stevens-Johnson syndrome (SJS) or toxic epidermal necrolysis (TEN), which can have a mortality rate as high as 40-50%. A multi-organ syndrome, manifested as fever, rash, eosinophilia, and hepatotoxicity, has also been reported in patients receiving these drugs (Dujovne et al., 1967; Berg, 1987; Rieder et al., 1989; Svensson et al., 2001).

Several studies have demonstrated that SMX and DDS undergo biotransformation to form reactive N-arylhydroxylamine metabolites (Figure 1), which are believed to be responsible for causing cutaneous drug reactions (CDRs) (Cribb et al., 1996a; Reilly and Ju, 2002; Svensson, 2003). It has been proposed that the bioactivation of these drugs at the site of manifestation (i.e., skin) may be a critical element in the initiation of these reactions (Reilly et al., 2000). Indeed, we have previously demonstrated that normal human epidermal keratinocytes (NHEK) are able

to bioactivate SMX and DDS to their respective arylhydroxylamine metabolites (SMX-NOH and DDS-NOH) (Reilly et al., 2000) and that such bioactivation results in protein haptenation (Roychowdhury et al., 2005).

Studies have demonstrated that skin cells express a variety of drug metabolizing enzymes, such as cytochromes P450 (CYP450s), cyclooxygenase (COX), flavin-containing monooxygenases (FMOs) and peroxidases, which may bioactivate numerous chemical agents (Kanekura et al., 1998; Rys-Sikora et al., 2000; Baron et al., 2001; Janmohamed et al., 2001; Saeki et al., 2002). Hydroxylation of SMX and DDS by various CYP450s has been reported (Cribb et al., 1995; Mitra et al., 1995; Gill et al., 1999; Winter et al., 2000). Several arylamine drugs, including procainamide, are oxidized to arylhydroxylamine metabolites by COX-2 (Liu and Levy, 1998; Goebel et al., 1999).

In the present investigation, we sought to identify the enzyme(s) that catalyze the bioactivation of SMX and DDS leading to protein haptenation in NHEK. Our studies demonstrate that while COX-1/2, CYP3A4 and CYP2E1 are able to catalyze the bioactivation of SMX and DDS *in vitro*, inhibitors of these enzymes do not reduce adduct formation when NHEK are exposed to either SMX or DDS. These data suggest that these enzymes do not play an important role in the bioactivation and subsequent protein adduction of SMX and DDS in NHEK.

METHODS

Materials. Monoacetyl dapsone (MADDS) was generously provided by Parke-Davis (now Pfizer, Ann Arbor, MI). DDS, SMX, 4-dimethylaminopyridine (DMAP), 1-aminobenzotriazole (ABT), troleandomycin, disulfiram and indomethacin (INDO) were obtained from Sigma (St. Louis, MO). 7-benzyloxyquinoline (7-BQ) and 7-hydroxyquinoline (7-HQ) were purchased from Gentest (Bedford, MA). DDS and SMX hydroxylamine metabolites were synthesized as described previously (Vyas et al., 2005). 1, 2-trans dichloroethylene (DCE) was obtained from TCI America (Portland, OR). Rabbit anti-sera was raised against SMX- and DDS-keyhole limpet hemocyanine conjugates and specificity assessed as described previously (Reilly et al., 2000). Rat tail collagen (type-I) was obtained from Sigma (St. Louis, MO). Normal human epidermal keratinocytes (as 1st passage cells) and keratinocyte culture media were obtained from CAMBREX (Walkersville, MD). HaCaT cell line was generated by Dr. N. Fusenig (DKFZ Heidelberg, Heidelberg, Germany) and obtained from Dr. Michael Southhall (Johnson & Johnson; Skillman, NJ). Microtiter ELISA plates (96 well) were obtained from Rainin Instruments (Woburn, MA). Rabbit anti-CYP2C9 antibody was custom made by Covance Research Products Inc. (Denver, PA). Donkey anti-rabbit IgG conjugated to horseradish peroxidase was obtained from Amersham Pharmacia Biotech Inc. (Piscataway, NJ). SuperSignal West Pico Chemiluminescent Substrate was purchased from Pierce (Rockford, IL) and a SynGene GeneGnome chemiluminescence detection system was obtained from Synoptics (Cambridge, UK). K03 monoclonal anti-CYP3A4 has been previously described (Beaune et al., 1985); rabbit α-3A5 primary antibody was purchased from Gentest. Goat-anti-rabbit IgG conjugated with Alexafluor 488 and

goat anti-rabbit antibody conjugated with alkaline phosphatase and YoYo-1 were purchased from Molecular Probes (Eugene, OR). Bradford assay reagent was purchased from Pierce Chemical Company (Rockford, IL). Immunomount was obtained from Vector Laboratories (Burlingame, CA). Trizol was purchased from Invitrogen (Carlsbad,CA). All other chemicals and reagents were purchased from Sigma (St. Louis, MO) or Fisher Scientific (Chicago, IL). Human liver microsomes were processed at St. Jude Children's Research Hospital and tissue was provided by the Liver Tissue Procurement and Distribution System (NIH Contract #N01-DK-9-2310 and by the Cooperative Human Tissue Network.

Synthesis of N-acetylsulfamethoxazole (NASMX). SMX (250 mg) was dissolved in 1 ml of acetic anhydride in presence of 0.5 g of DMAP and 10 ml of dichloromethane. The reaction was carried out for 1 h at room temperature with continuous stirring to obtain NASMX. Excess of acetic anhydride was removed by neutralizing the reaction mixture with saturated sodium bicarbonate solution and NASMX obtained by re-crystallizing the product in an acetone and hexane (1:3) mixture. NASMX was characterized by NMR and the purity was determined by HPLC-UV. Product purity was 98% while the observed yield was 79%.

Cell Culture. Adult normal human keratinocytes (NHEK) and immortalized HaCaT cells were cultured as detailed previously (Reilly et al., 2000). In brief, cells were propagated in 75 cm^2 flasks using basal media (KBM-2) supplemented with bovine pituitary extract (7.5 mg/ml), human epidermal growth factors (0.1 ng/ml), insulin (5 μg/ml), hydrocortisone, (0.5 μg/ml), epinephrine, transferrin, gentamicin (50 μg/ml) and amphotericin (50 ng/ml) at 37°C in an atmosphere containing 5% CO_2. Media was

replaced every 2-3 days. When cell cultures reached near confluency (70-90%), cells were disaggregated using 0.025% Trypsin/0.01% EDTA in HEPES followed by neutralization with 2 volumes of Trypsin neutralizing solution. Cell suspensions were then centrifuged at 220 x g for 5 min followed by washing in basal media and re-suspension in KGM-2 (Supplemented growth medium). Cells were then either subjected to subculturing or cryo-preservation for further purposes. All experiments were performed using 3rd to 4th passage cells.

Determination of mRNA for CYP2C9 in NHEK. Total RNA was isolated from 4th passage NHEK and 7th passage HaCaT cells using Trizol (Invitrogen) following the manufacturer's protocol. cDNA was generated using 500 ng total RNA in a synthesis reaction using SuperScript™ II RT with random hexamers according to the supplier's protocol. PCR was performed using the CYP2C9 specific primers 5'-GATCTGCAATAATTTTTCTC-3' and 5'-TCTCAGGGTTGTGCTTGTC-3' with diluted amounts of cDNA from the keratinocytes resulting in a 280 bp product. Plasmid CYP2C9 cDNA in pCW was used as a positive control for amplification. Actin was also amplified from the keratinocyte cDNA using the primers 5'-TCATGAAGTGTGACGTTGACATCCGT-3' and 5'-CCTAGAAGCATTTGCGGTGCACGATG-3' resulting in a 285 bp fragment. Amplifications were performed in 20 µl reactions using Amplitaq Gold (Applied Biosystems) according to the manufacturer's protocol with a final concentration of $MgCl_2$ of 2 mM. Cycling conditions consisted of an initial denaturation at 94° for 5 min followed by 40 cycles of 94° for 30 s, 53° for 10 s and 72° for 10 s. Reactions were analyzed on 4% agarose gels stained with ethidium bromide.

Immunoblot analysis for CYP2C proteins in NHEK. Cell lysates and yeast-expressed recombinant CYP2C proteins were fractionated by electrophoresis in SDS-10% (w/v) polyacrylamide gels and transferred to nitrocellulose membranes. Membranes were immunoblotted with a polyclonal rabbit anti-CYP2C9 antibody (1:500) raised to bacterially expressed human CYP2C9 and donkey anti-rabbit IgG conjugated to horseradish peroxidase. This anti-CYP2C9 polyclonal antibody to bacterially expressed recombinant CYP2C9 was made for NIEHS by Covance (Denver, Pennsylvania) using a standard NIEHS rabbit antibody production protocol. Yeast expressed CYP2C proteins were utilized as standards on immunoblots, since there is no N-terminal modification for cDNA expression in yeast. Therefore, the recombinant yeast-expressed CYP2C proteins have mobilities identical to those of the human CYP proteins expressed *in vivo*. Specific bands were visualized with SuperSignal West Pico Chemiluminescent Substrate and a SynGene GeneGnome chemiluminescence detection system.

Determination of mRNA for CYP3A4 and CYP3A5 in NHEK. Total RNA was isolated from NHEK and HaCaT cells using Trizol Reagent (Invitrogen) and first strand cDNA was synthesized from 3 µg of total RNA according to the manufacturer's instructions (SuperScript First Strand cDNA Synthesis kit, Invitrogen). Amplification of CYP3A4 cDNA (Genbank no. AF182273) from first strand cDNA was performed using (f) 5'-CCCAGACTTG GCCATGGAAACC-3' and (r) 5'-GAGGTCTCTGGTGTTCTCAG-3' primers that annealed to nucleotides in exon 1 and 13. PCR was carried out in a total reaction volume of 50 µl consisting of 5 × PCR buffer with 1.5 mM $MgCl_2$, 1 µl , 5 pmol of each primer, 0.2 mM dNTP (Life Technologies, Gaithersburg, MD, USA), and 2.5 U of

Taq DNA Polymerase (Boehringer Mannheim Expand High Fidelity PCR system, Mannheim, Germany). PCR consisted of at initial denaturation at 94 °C for 3 min followed by 35 cycles of denaturation at 94 °C for 30 s, annealing at 55 °C for 30 s and synthesis at 72 °C for 90 s and a final extension at 72 °C for 10 min. No CYP3A4 was detected, so an aliquot of the first round product was PCR amplified for a second round with the same primers and conditions to detect if very small amounts of mRNA were present. CYP3A5 was amplified using (P1-f) 5'−AACAGCCCAGCAAACAGCAGC−3' (f), and (P2-r), 5'−TAAGCCCATCTTTATTTCAAGGT−3' primers as described previously (Kuehl et al., 2001) and product was detected after the first round amplification.

Determination of protein for CYP3A4 and CYP3A5 in NHEK. NHEK, HaCaT cell and human liver samples were resuspended in storage buffer (100 mM potassium phosphate, pH 7.4, 1.0 mM EDTA, 20% glycerol, 1 mM dithiothreitol, 20 µM butylated hydroxytoluene, 2 mM phenylmethylsulfonyl fluoride), lysates were generated by sonication, and protein concentrations determined using the Bio-Rad protein assay. 30 µg of lysate was separated on 10% SDS-polyacrylamide gels and immunoblotted with monoclonal anti-CYP3A4 K03 or rabbit α-3A5 (Gentest), followed by appropriate secondary antibodies coupled with peroxidase. The blot was developed with the ECL detection system (Amersham Biosciences).

Determination of catalytic activity for CYP3A4 in NHEK. NHEK (10^6 cells) were incubated in KGM-2 overnight. After 24 h, the media was discarded and replaced with fresh media. 7-Benzyloxyquinoline (7-BQ; 50 µM), a substrate for CYP3A4, was added to measure the catalytic activity of CYP3A4 in these cells. The plate was incubated for 30 min at 37°C after the addition of 7-BQ followed by the fluorescence measurement

JPET Fast Forward. Published on July 20, 2006 as DOI: 10.1124/jpet.106.105858
This article has not been copyedited and formatted. The final version may differ from this version.

every 30 min for 24 h using the Cytofluor multiwell fluorescent plate reader (excitation wavelength of 410 nm and emission wavelength of 538 nm). The fluorescent metabolite of 7-BG, 7-hydroxyquinoline (7-HQ), was also added to NHEK at varying concentrations (0, 5, 10, 25 and 50 µM) to determine the ability to detect this metabolite in the presence of NHEK.

Determination of CYP2E1 in NHEK. CYP2E1 mRNA expression was quantified in NHEK and HaCaT cells essentially as described by Haufroid et al (Haufroid et al., 2001). Briefly, total RNA was isolated from keratinocytes using Trizol reagent (Invitrogen, Carlsbad, CA) and quantified using a Quant-iT RiboGreen kit (Invitrogen) as per the manufacturer's instructions. Using 2 µg of total RNA from each cell preparation, cDNA was prepared using random hexamer primers and ImProm-II reverse transcriptase following the procedures outlined in the ImProm-II Reverse Transcription System kit (Promega, Madison, WI). RT-PCR reactions to quantify CYP2E1 mRNA concentrations were carried out in a total volume of 40 µl containing 5.5 mM $MgCl_2$, 0.2 mM each deoxyribonucleotide, 0.3 µM of each PCR primer and 0.2 µM fluorescent probe, 5 or 25 ng of keratinocyte cDNA, 0.01 U/µl uracil N-glycosylase and 0.025 U/µl AmpliTaq Gold Polymerase (TaqMan PCR Core Reagents kit, Applied Biosystems, Foster City, CA) in a MJ Research Opticon System (MJ Research, Watertown, MA). 18S rRNA concentrations were determined using the TaqMan Ribosomal RNA Control Reagents (ABI) which were designed to generate a 187 bp product. Each 40 µl PCR reaction contained 5.5 mM $MgCl_2$, 0.2 mM each deoxyribonucleotide, 0.05 µM of each PCR primer and 0.2 µM fluorescent probe, 5 or 25 ng of keratinocyte cDNA, 0.01 U/µl

uracil N-glycosylase and 0.025 U/µl AmpliTaq Gold Polymerase (TaqMan PCR Core Reagents kit, ABI).

Determination of the Cytotoxicity of Inhibitors in NHEK. To determine the maximal non-cytotoxic concentrations of various inhibitors in NHEK for the inhibition of the respective enzymes, the cytotoxicity of concentrations ranging from 25 µM to 25 mM were examined. Cytotoxicity was determined using an impermeable DNA binding dye (YoYo - 1), as we have described previously (Vyas et al., 2005).

ELISA Analysis of Drug/metabolite-protein Adducts. Formation of covalent adducts following SMX or DDS exposure, in the presence or absence of the selective enzyme inhibitors, was determined by cultivating NHEK (1 X 10^6 cells) for 24 h in 50 ml centrifuge tubes containing 10 ml of complete growth medium. The concentrations of the selective inhibitors used were the maximum non-cytotoxic concentrations of those inhibitors in NHEK. Cells were then incubated with selective enzyme inhibitors for 3 h followed by SMX (1 mM ascorbic acid was added prior to the addition of SMX) or DDS treatment for 3 h (concentrations specified in Results). Following total 6 h incubation, tubes were centrifuged at 220 x g for 5 min to pellet the cells. Covalent adducts were determined as previously described (Vyas et al., 2005).

Immunocytochemistry. Drug/metabolite-protein covalent adduct formation was visualized using immunofluorescence confocal microscopy. Cells were grown on collagen-coated (0.1 mg/ml) coverslips placed in Petri-dishes containing 2 ml of complete growth medium. After 24 h, cultures were subjected to different selective enzyme inhibitors for 3 h (maximum non-cytotoxic concentrations were used), followed by SMX or DDS treatment for 3 h (concentrations specified in Results). After the 3 h

incubation, cells were washed (three times) with phosphate buffered saline (PBS, 0.05M sodium phosphate, 0.15M NaCl, pH 7.4) and fixed for 20 min with 4% paraformaldehyde (PFA) in PBS. After fixation, cultures were washed 3 times with PBS followed by blocking for 60 min with Tris-casein buffer containing 0.3% Triton-X-100 and overnight incubation with the anti-DDS or anti-SMX antisera (1:500 diluted in blocking buffer) at 4^{o}C. Coverslips were then washed with PBS, incubated for 3 h at 37^{o}C with the fluorochrome-conjugated secondary antibody (Alexa fluor-488 labeled goat-anti-rabbit IgG, 1:500 diluted in blocking buffer), and mounted on glass slides using Immunomount® containing anti-fade reagent.

Fluorescence images were acquired with a Zeiss Laser Scanning Microscope (LSM 510, Zeiss Axiovert stand, Zeiss 63x and 20x objective lens) using excitation at 488 nm. Emission was set to a long pass filter at 505 nm.

Image analysis. For imaging with the confocal laser scanning microscope, laser attenuation, pinhole diameter, photomultiplier sensitivity and offset were kept constant for every set of experiments. Images were acquired from 3 different view fields of each slide. The obtained images were quantitatively analyzed for changes in fluorescence intensities within regions of interests (boxes drawn over cell somata) using the Image J software. Fluorescence values from minimum of 3 view fields consisting of 15-20 NHEK cells in each field from 3 different slides of each treatment were averaged and expressed as mean (SD) fluorescence intensity.

Statistical analysis. Data are presented as mean (SD). Data were analyzed using SIGMASTAT (USA). Statistical comparisons between two groups were made using either student t-test (parametric method) for normalized data or Friedman's rank sum

test (nonparametric method) for the data which did not pass the normality test. For the comparison between more than two groups, ANOVA and the Holm-Sidak method for multiple pairwise comparisons was used. A value of $p<0.05$ was considered to be significant.

RESULTS

Covalent adduct formation of DDS and SMX and their acetylated metabolites in NHEK. Protein haptenation of the parent arylamine drugs, DDS and SMX, was readily detected by both confocal microscopy and ELISA (Fig. 2 and 3). N-acetylation of SMX or DDS resulted in marked attenuation of protein haptenation. As we have noted previously, the amount of adduct formed with DDS appears to be greater than that seen with SMX, though this may represent differences in antisera affinity for the respective adducts.

Expression of various cytochromes P450 in keratinocytes. NHEK and an immortalized keratinocyte cell line (HaCaT) were probed for the presence of various CYP450s known to catalyze the formation of the arylhydroxylamine metabolites of SMX and DDS *in vitro*. As shown in Fig. 4, CYP2C9 mRNA was not detected in cells from cultures of primary keratinocytes (NHEK) and HaCaT cells using multiple dilutions of cDNA. However, immunoblot analysis suggested the possible presence of CYP2C9 (a diffuse polypeptide band with approximately the same mobility as recombinant CYP2C9) in the first sample of NHEK, but which was not seen in the second sample of cells from the same patient or in HaCaT cells. Moreover, CYP2C8, CYP2C18, or CYP2C19 were not detected in either cell type (Fig. 5). The recombinant CYP2C protein standards were expressed in a yeast cDNA expression system as described previously (Goldstein et al., 1994). Interestingly, while both CYP3A4 and CYP3A5 mRNA were observed in NHEK, only CYP3A5 mRNA was observed in HaCaT cells (Fig. 6A). Immunoblot analysis using an antibody specific for CYP3A5 yielded positive results in both NHEK and HaCaT cells, as did an antibody that recognizes both CYP3A4 and

CYP3A5 (Fig. 6B). However, the levels of CYP3A4 and CYP3A5 proteins were much lower as compared to the human livers. CYP2E1 mRNA was also found to be expressed in both NHEK and HaCaT cells (Fig. 7), while CYP2E1 protein was barely detectable (data not shown).

CYP3A4 activity in NHEK. After addition of 7-BQ, no increase in fluorescence above background (NHEK alone) was observed (data not shown). In contrast, a concentration-dependent increase in fluorescence was observed when the expected metabolite (7-HQ) was added to NHEK (data not shown) – indicating the metabolite is readily detected down to 5 μM in NHEK incubations.

Covalent adduct formation of DDS and SMX in presence and absence of inhibitors of various enzymes. The effect of various enzyme inhibitors on protein haptenation in NHEK exposed to SMX or DDS was evaluated by both confocal microscopy and ELISA. For each inhibitor, we utilized the highest concentration that did not cause cytotoxicity in NHEK. As shown in Fig. 8, a broad inhibitor of CYP450 (ABT) which inhibits CYP3A4 and CYP2C9, a selective inhibitor of CYP2E1 (DCE), and an inhibitor of COX (INDO) failed to reduce the protein haptenation of DDS in NHEK cells. Similar results were observed with SMX by ELISA (Fig. 9). Similar results were obtained when inhibitors were added simultaneously with SMX or DDS and incubated for 3 h (data not shown). We also found that troleandomycin (a potent inhibitor of CYP3A4) and disulfiram (CYP2E1 inhibitor) did not attenuate the protein haptenation with either DDS or SMX (data not shown).

DISCUSSION

The biotransformation of xenobiotics to reactive metabolites is believed to be responsible for a wide range of adverse reactions. Sulfonamides such as SMX and the sulfone DDS have been reported to be bioactivated to arylhydroxylamine metabolites, which readily autooxidize to arylnitroso species (Fig. 1). These metabolites are believed to initiate the cascade of events that ultimately provoke a CDR (Cribb et al., 1996b; Svensson, 2003). We have previously proposed that bioactivation in the skin may play an important role in these reactions (Reilly et al., 2000). Indeed, incubation of NHEK with SMX or DDS results in protein haptenation (Roychowdhury et al., 2005)

In vitro studies have shown that the bioactivation of these parent arylamine drugs to their arylhydroxylamine metabolites may be mediated by various oxidizing enzymes such as CYP2C9, CYP2E1, CYP3A4, and MPO (Cribb et al., 1990; Uetrecht, 1990; Cribb et al., 1995; Mitra et al., 1995; Gill et al., 1999; Winter et al., 2000). Several arylamine drugs, including procainamide, are oxidized to arylhydroxylamine metabolites by COX-2 *in vitro* (Liu and Levy, 1998; Goebel et al., 1999). Which of these enzymes, if any, mediates the bioactivation of SMX and DDS in NHEK is unknown.

To assess the importance of arylamine oxidation, we evaluated the impact of SMX and DDS N-acetylation on protein haptenation in NHEK. We found that the N-acetyl metabolites gave rise to a lower level of protein haptenation as measured by both ELISA and confocal microscopy (Fig. 2 and 3). It should be noted that it is possible that the apparent reduction in adduct formation could be secondary to a reduced affinity of the antisera for the adduct in the presence of an acetyl group on the drug, as opposed to an actual reduction in the amount of adduct formed. Differentiation of these two

potential explanations could only be accomplished by the characterization of and development of chemical methods for the quantification of the drug-protein adducts.

Prior to evaluating the effect of various enzyme inhibitors on protein haptenation with these drugs, we sought to confirm the presence of the most probable enzymes for bioactivation in NHEK. As HaCaT cells are widely used as an alternative to primary cultures of NHEK, together with our previous observation of protein haptenation in these cells when exposed to SMX or DDS (Roychowdhury et al., 2005), we also examined the presence of CYP450 enzymes in this cell line. CYP2C9 appears to be the most important enzyme for bioactivating SMX and DDS in the human liver (Cribb et al., 1995; Gill et al., 1999; Winter et al., 2000). We did observe a polypeptide band with the approximate mobility of recombinant CYP2C9 in the one sample of NHEK. This band was not seen in a second sample of NHEK from the same patient or in either shipment of HaCaT cells. In addition, there was no evidence of other members of the CYP2C family of enzymes in either NHEK or HaCaT cells when probed by immunoblot. Moreover, we did not detect the presence of CYP2C9 message in either cell type (Fig. 4). Yengi et al (Yengi et al., 2003) have previously reported the expression of CYP2C9, CYP2C18, and CYP2C19 transcripts in human skin samples. As these investigators probed full thickness skin, it is not possible to determine which skin cells gave rise to these transcripts. Saeki et al (Saeki et al., 2002) have observed the presence of CYP2C transcripts in human keratinocytes from several subjects. However, their use of non-specific primers does not permit identification of the specific CYP2C genes that were expressed in these cells. Moreover, transcripts can be detected in the absence of detectable protein. While our data suggest the possible presence of a low level of

CYP2C9 protein in NHEK, further studies are needed to more carefully determine the expression of this enzyme in human skin.

The results shown in Fig. 6 suggest that CYP3A5 is the protein detected in both NHEK and HaCaT cells, as it was detected by an antibody that is immunospecific for CYP3A5. Moreover, CYP3A5 mRNA was readily amplified from NHEK and HaCaT cells, while a second round of PCR amplification was required to detect CYP3A4 mRNA transcript in NHEK cells (Fig. 6B). To our knowledge, this differential expression of CYP3A enzymes has not been demonstrated previously in keratinocytes. The differential expression of CYP3A4/5 proteins, especially much lower expression in NHEK and HaCaT cells as compared to liver, might suggest the minor role of these enzymes for the bioactivation of these parent drugs in skin. Interestingly, we were unable to demonstrate the metabolism of a CYP3A4 substrate (7-BQ) in NHEK, though its metabolite (7-HQ) was readily detected when added directly to NHEK. This suggests a very low level of CYP3A4-mediated catalytic activity in these cells. We were also able to demonstrate the presence of CYP2E1 mRNA in both NHEK and HaCaT cell types (Fig. 7). This is consistent with the reports of other investigators who have demonstrated the presence of CYP2E1 transcripts and protein in NHEK (Saeki et al., 2002, Baron et al., 2001).

Based on the mRNA and protein data, we concluded that CYP2C9 was not a likely mediator of the bioactivation of these drugs in NHEK. Indeed, preliminary studies demonstrated that sulfaphenazole, an inhibitor of CYP2C9, did not inhibit protein haptenation in NHEK exposed to SMX or DDS (Wurster et al., 2004).To evaluate the role of CYP3A4/5 and CYP2E1 in the generation of drug-protein adducts, we evaluated

the effect of inhibitors of these enzymes (at their maximum non-cytotoxic concentration) on protein haptenation in NHEK exposed to SMX or DDS. Our results indicate that a general inhibitor of CYP450s, ABT (which has been shown to completely (~ 90%) inhibit most of the major CYP450s, such as CYP1A2, 2B6, 2C9, 2C19, 2D6, and 3A4) (Balani et al., 2002), did not reduce the covalent adducts formed after exposure of NHEK to DDS and SMX (Fig. 8 and 9). The selective inhibitor of CYP2E1 (DCE) also failed to decrease adduct formation. Other inhibitors of CYP3A4 (troleandomycin) and CYP2E1 (disulfiram) also did not reduce the protein haptenation of DDS and SMX in NHEK (data not shown). These results suggest that CYP450 does not play a major role in the oxidative metabolism of these drugs in NHEK. In addition, though COX-2 has been shown to mediate the oxidation of arylamines *in vitro*, an inhibitor of cyclooxygenase (indomethacin) did not attenuate the protein haptenation in NHEK exposed to either DDS or SMX (Fig. 8 and 9). This is consistent with our recent observation that recombinant COX-2 does not mediate the oxidation of these drugs (Vyas et al., 2006).

Hence, our studies confirm our previous observations that NHEK are able to bioactivate SMX and DDS giving rise to haptenated proteins. We found that CYP450s that are important in the bioactivation of these drugs in the liver do not appear to play a significant role in their bioactivation in NHEK. It should be noted, however, that recent data suggests the level of CYP450 expression may differ as keratinocytes differentiate (Du et al., 2006). Nevertheless, we observed significant protein haptenation in NHEK in the absence of evidence for involvement of CYP450. These studies demonstrate that the role of various drug metabolizing enzymes in the bioactivation of drugs may vary from tissue to tissue. Likewise, though COX-2 has been reported to oxidize arylamines,

neither COX-1 nor COX-2 appears to contribute to the bioactivation of these drugs in NHEK. In our companion paper to this current investigation, we demonstrate the role of FMO and peroxidases in the bioactivation of these arylamine drugs in keratinocytes.

ACKNOWLEDGEMENTS

The authors wish to acknowledge the assistance of Mr. William Wurster and Dr. Radita Nemes in conducting preliminary studies in support of this project. We also wish to thank the staff of the Central Microscopy Research Facility at The University of Iowa, which is supported by the Office of the Vice President for Research, for their technical assistance.

REFERENCES

Balani SK, Zhu T, Yang TJ, Liu Z, He B and Lee FW (2002) Effective dosing regimen of 1-aminobenzotriazole for inhibition of antipyrine clearance in rats, dogs, and monkeys. *Drug Metab Dispos* **30**:1059-1062.

Baron JM, Holler D, Schiffer R, Frankenberg S, Neis MMH and Jugert FK (2001) Expression of multiple cytochrome p450 enzymes and multidrug. *J Invest Dermatol* **116**:541-548.

Beaune P, Kremers P, Letawe-Goujon F and J.E. Gielen (1985) Monoclonal antibodies against human liver cytochrome P-450. *Biochem Pharmacol* **34**:3547-3552.

Berg PA, Daniel PT (1987) Co-trimoxazole-induced liver injury - an analysis of cases with hypersensitivity-like reactions. *Infection* **15**:S259-S263.

Cribb AE, Lee BL, Trepanier LA and Spielberg SP (1996a) Adverse reactions to sulphonamide and sulphonamide-trimethoprim antimicrobials: clinical syndromes and pathogenesis. *Adv Drug React Toxicol Rev* **15**:9-50.

Cribb AE, Miller M, Tesoro A and Spielberg SP (1990) Peroxidase-dependent oxidation of sulfonamides by monocytes and neutrophils from humans and dogs. *Mol Pharmacol* **38**:744-751.

Cribb AE, Nuss CE, Alberts DW, Lamphere DB, Grant DM, Grossman SJ and Spielberg SP (1996b) Covalent binding of sulfamethoxazole reactive metabolites to human and rat liver subcellular fractions assessed by immunochemical detection. *Chem Res Toxicol* **9**:500-507.

Cribb AE, Spielberg SP and Griffin GP (1995) N4-hydroxylation of sulfamethoxazole by cytochrome P450 of the cytochrome P4502C subfamily and reduction of

sulfamethoxazole hydroxylamine in human and rat hepatic microsomes. *Drug Metab Dispos* **23**:406-414.

Du L, Neis MM, Ladd PA, Lanza DL, Yost GS and Keeney DS (2006) Effects of the differentiated keratinocyte phenotype on expression levels of CYP1-4 family genes in human skin cells. *Toxicol Appl Pharmacol* **213**:135-144.

Dujovne D, Chan C and Zimmerman H (1967) Sulfonamide hepatic injury. *N Engl J Med* **377**:785-788.

Gill HJ, Tija J, Kitteringham NR, Pirmohamed M, Back DJ and Park BK (1999) The effect of genetic polymorphism in CYP2C9 on sulphamethoxazole N-hydroxylation. *Pharmacogenetics* **9**:43-53.

Goebel C, Vogel C, Wulferink M, Mittmann S, Sachs B, Schraa S, Abel J, Degen G, Uetrecht J and Gleichmann E (1999) Procainamide, a drug causing lupus, induces prostaglandin H synthase-2 and formation of T cell-sensitizing drug metabolites in mouse macrophages. *Chem Res Toxicol* **12**:488-500.

Goldie SJ, Kaplan JE, Losina E, Weinstein MC, Paltiel AD, Seage GR, Craven DE, Kimmel AD, Zhang H, Cohen CJ and Freedberg KA (2002) Prophylaxis for human immunodeficiency virus-related Pneumocystis carinii pneumonia: using simulation modeling to inform clinical guidelines. *Arch Intern Med* **162**:921-928.

Goldstein JA, Faletto MB, Romkes-Sparkes M, Sullivan T, Kitareewan S, Raucy JL, Lasker JM and Ghanayem BI (1994) Evidence that CYP2C19 is the Major (S)-Mephenytoin 4'-hydroxylase in humans. *Biochemistry* **33**:1743-1752.

Haufroid V, Toubeau F, Clippe A, Buysschaert M, Gala JL and Lison D (2001) Real-time quantification of cytochrome P4502E1 mRNA in human peripheral blood

lymphocytes by reverse transcription-PCR: method and practical application. *Clin Chem* **47**:1126-1129.

Hughes WT (1987) Treatment and prophylaxis for Pneumocystis carinii pneumonia. *Parasitol Today* **3**:332-335.

Janmohamed A, Dolphin CT, Phillips IR and Shephard EA (2001) Quantification and cellular localization of expression in human skin of genes encoding flavin-containing monooxygenases and cytochromes P450. *Biochem Pharmacol* **62**:777-786.

Kanekura T, Laulederkind SJF, Kirtikara K, Goorha S and Ballou LR (1998) Cholecalciferol induces prostaglandin E2 biosynthesis and transglutaminase activity in human keratinocytes. *J Invest Dermatol* **111**:634-639.

Kuehl P, Zhang J, Lin Y, Lamba J, Assem M, Schuetz J, Watkins PB, Daly A, Wrighton SA, Hall SD, Maurel P, Relling M, Brimer C, Yasuda K, Venkataramanan R, Strom S, Thummel K, Boguski MS and Schuetz E (2001) Sequence diversity in CYP3A promoters and characterization of the genetic basis of polymorphic CYP3A5 expression. *Nat Genet* **27**:383-391.

Liu Y and Levy GN (1998) Activation of heterocyclic amines by combinations of prostaglandin H synthase-1 and -2 with N-acetyltransferase 1 and 2. *Cancer Lett* **133**:115-123.

Mitra AK, Thummel KE, Kalhorn TF, Kharasch ED, Unadkat JD and Slattery JT (1995) Metabolism of dapsone to its hydroxylamine by CYP2E1 in vitro and in vivo. *Clin Pharmacol Ther* **58**:556-566.

Reilly TP, Lash LH, Doll MA, Hein DW, Woster PM and Svensson CK (2000) A role for bioactivation and covalent binding within epidermal keratinocytes in sulfonamide-induced cutaneous drug reactions. *J Invest Dermatol* **114**:1164-1173.

Reilly TP and Ju C (2002) Mechanistic perspectives on sulfonamide-induced cutaneous drug reactions. *Curr Opin Allergy Clin Immunol* **2**:307-315.

Rieder MJ, Uetrecht J, Shear NH, Cannon M, Miller M and Spielberg SP (1989) Diagnosis of sulfonamide hypersensitivity reactions by in-vitro "rechallenge" with hydroxylamine metabolites. *Ann Intern Med* **110**:286-289.

Roychowdhury S, Vyas PM, Reilly TP, Gaspari AA and Svensson CK (2005) Characterization of the formation and localization of sulfamethoxazole and dapsone-associated drug-protein adducts in human epidermal keratinocytes. *J Pharmacol Exp Ther* **314**:43-52.

Rys-Sikora KE, Konger RL, Schoggins JW, Malaviya R and Pentland AP (2000) Coordinate expression of secretory phospholipase A2 and cyclooxygenase -2 in activated human keratinocytes. *Am J Physiol Cell Physiol* **278**:C822-C833.

Saeki M, Saito Y, Nagano M, Teshima R, Ozawa S and Sawada JI (2002) mRNA expression of multiple cytochrome P450 isozymes in four types of cultured skin cells. *Int Arch Allergy Immunol* **127**:333-336.

Svensson CK (2003) Do arylhydroxylamine metabolites mediate the idiosyncratic reactions associated with sulfonamides and sulfones? *Chem Res Toxicol* **16**:1034-1043.

Svensson CK, Cowen EW and Gaspari AA (2001) Cutaneous drug reactions. *Pharmacol Rev* **53**:357-379.

Uetrecht JP (1990) Drug metabolism by leukocytes and its role in drug-induced lupus and other idiosyncratic drug reactions. *Crit Rev Toxicol* **20**:213-235.

Vyas PM, Roychowdhury S and Svensson CK (2006) Role of human cyclooxygenase-2 in the bioactivation of dapsone and sulfemethoxazole. *Drug Metab Dispos* 34:16-18.

Vyas PM, Roychowdhury S, Woster PM and Svensson CK (2005) Reactive oxygen species generation and its role in the differential cytotoxicity of the arylhydroxylamine metabolites of sulfamethoxazole and dapsone in normal human epidermal keratinocytes. *Biochem Pharmacol* **70**:275-286.

Winter HR, Wang Y and Unadkat JD (2000) CYP 2C8/9 mediate dapsone N-hydroxylation at clinical concentrations of dapsone. *Drug Metab Dispos* **28**:865-868.

Wurster W, Nemes R, Lamba J, Schuetz EG, Blaisdell J, Goldstein JA, Reilly TP and Svensson CK (2004) Bioactivation of sulfamethoxazole (SMX) and dapsone (DDS) in normal human epidermal keratinocytes (NHEK) results in the formation of drug-protein adducts. *Allergologie* **4**:169.

Yengi LG, Xiang Q, Pan J, Scatina J, Kao J, Ball SE, Fruncillo R, Ferron G and Wolf CR (2003) Quantitation of cytochrome P450 mRNA levels in human skin. *Anal Biochem* **316**:103-110.

FOOTNOTES

This work was supported in part by NIH Grants AI41395 and GM63821 to CKS, and GM60346 to EGS.

Legends for Figures

Figure 1. Scheme for the bioactivation of SMX and DDS giving rise to protein haptenation. Abbreviations: COX – cyclooxygenase; CYP450s – cytochromes P450; MPO – myeloperoxidase; NAT – N-acetyltransferase**.**

Figure 2. Protein haptenation in NHEK incubated with DDS or MADDS. A. NHEK were incubated in the presence of vehicle (1% DMSO) or 800 µM of DDS or MADDS for 24 h. Cells were then imaged using confocal microscopy (objective lens: 20x) as described in Materials and Methods. Micrographs are representative images from each incubation condition. **B.** Images for control, DDS and MADDS in figure 2A were analyzed by Image J software and fluorescence intensity from a minimum of 3 view fields of 3 different slides of each treatment (with 15 – 20 cells per field) were averaged and expressed as mean (SD) fluorescence intensity (arbitrary units). Results were analyzed using ANOVA with the Holm-Sidak method for multiple pairwise comparisons. $^{*}p < 0.05$ compared to control; $^{**}p < 0.05$ compared to control or MADDS. **C.** Determination of covalent adducts of DDS and MADDS (800 µM, 24h) in NHEK by ELISA as described in Materials and Methods. Data presented represent the mean (SD) optical density of three different experiments having three replicates in each experiment. Data were analyzed using ANOVA with the Holm-Sidak test for multiple pairwise comparisons. $^{*}p< 0.05$ compared to NHEK incubated with vehicle or MADDS.

Figure 3. Protein haptenation in NHEK incubated with SMX or NASMX. A. NHEK were incubated in the presence of vehicle (1% DMSO) or 800 µM of SMX or NASMX for

24 h. Cells were then imaged using confocal microscopy (objective lens: 63x) as described in Materials and Methods. Micrographs are representative images from each incubation condition. **B.** Images for control, SMX and NASMX in figure 3A were analyzed by Image J software and fluorescence intensity from a minimum of 3 view fields of 3 different slides of each treatment (with 5 – 10 cells per field) were averaged and expressed as mean (SD) fluorescence intensity (arbitrary units). Results were analyzed using ANOVA with the Holm-Sidak method for multiple pairwise comparisons. $^{*}p < 0.05$ compared to control and NASMX. **C.** Determination of covalent adducts of SMX and NASMX (800 µM, 24h) in NHEK by ELISA as described in Materials and Methods. Data presented represent the mean (SD) optical density of three different experiments having three replicates in each experiment. Data were analyzed using ANOVA with the Holm-Sidak test for multiple pairwise comparisons. $^{*}p< 0.05$ compared to NHEK incubated with vehicle or NASMX.

Figure 4. Blot Gel analysis of PCR products for CYP2C9 mRNA expression in NHEK and HaCaT cells. 4th passage NHEK (designated as 4^NHEK) and HaCaT (designated 7^HaCaT) cells were probed for mRNA expression using CYP2C9 specific primers, as described in Materials and Methods. Various dilutions of the cDNA were evaluated as denoted. Note the absence of a band in both cell types corresponding to CYP2C9.

Figure 5. Immunoblot analysis for CYP2C9 protein expression in NHEK and HaCaT cells. 4th passage NHEK and HaCaT cells were fractionated by electrophoresis

on SDS-polyacrylamide gels as described in Methods and probed for CYP2C proteins using a polyclonal antibody to CYP2C9, which recognizes all of the human CYP2C proteins. Replicate sets of cells were analyzed (designated as 1st and 2nd shipment). YE stands for Yeast expressed (recombinant proteins).

Figure 6. A) RT-PCR analysis for CYP3A4 and CYP3A5 mRNA expression in NHEK and HaCaT cells. 4th passage NHEK and HaCaT cells were probed for mRNA expression using CYP3A4 and CYP3A5 specific primers and the products resolved on agarose gels as described in Materials and Methods. Note the absence of CYP3A4 mRNA in HaCaT cells. **B) Immunoblot analysis for CYP3A expression in NHEK, HaCaT cells and human livers.** 4th passage NHEK, HaCaT cells and human livers were probed for CYP3A proteins using a monoclonal antibody that recognizes both CYP3A4 and CYP3A5 or an anti-CYP3A5 specific antibody. Human liver microsomes from a CYP3A5 expressor (right) and a non-expressor (left) were run as positive controls.

Figure 7. Quantitative RT-PCR assessment of CYP2E1 mRNA in NHEK and HaCaT cells. CYP2E1 mRNA was quantified in NHEK and HaCaT cells as described in Materials and Methods. CYP2E1 mRNA was normalized to 18S rRNA. NHEK represent data from 2nd passage cells from one patient (Subject 1) and 3rd passage cells from a different patient (Subject 2).

Figure 8. Protein haptenation of DDS in NHEK in the presence of inhibitors of CYP450s and cyclooxygenase. NHEK were incubated for 3 h in the presence of vehicle (1% DMSO), 5 mM aminobenzotriazole (ABT), 5 mM trans-dichloroethylene (DCE), or 100 µM indomethacin (INDO). The concentrations of inhibitors selected were the maximal concentrations that did not increase cell death in NHEK under the incubation conditions. After pre-incubation with inhibitors, cells were incubated for an additional 3 h with 250 µM DDS. Covalent adducts were quantified using confocal microscopy (A) or ELISA (B), as described in Materials and Methods. **A.** Quantification of adducts was performed as described in Materials and Methods. Control represents NHEK incubated with vehicle (1% DMSO) alone. Results were analyzed using ANOVA with Holm-Sidak method for multiple pairwise comparisons. $^{*}p < 0.05$ compared to NHEK incubated with vehicle alone. **B.** Covalent adducts were determined by the ELISA as described in Materials and Methods. Data presented represent the mean (SD) optical density of three different experiments having three replicates in each experiment. Data were analyzed statistically using ANOVA with the Holm-Sidak test for multiple pairwise comparisons. $^{*}p< 0.05$ compared to NHEK incubated with vehicle alone.

Figure 9. Protein haptenation of SMX in NHEK in the presence of inhibitors of CYP450s and cyclooxygenase. NHEK were incubated for 3 h in the presence of vehicle (1% DMSO), 5 mM aminobenzotriazole (ABT), 5 mM trans-dichloroethylene (DCE), or 100 µM indomethacin (INDO). The concentrations of inhibitors selected were the maximal concentrations that did not increase cell death in NHEK under the incubation conditions. After pre-incubation with inhibitors, cells were incubated for an

additional 3 h with 250 µM SMX. Covalent adducts were quantified using ELISA as described in Materials and Methods. Data presented represent the mean (SD) optical density of three different experiments having three replicates in each experiment. Data were analyzed statistically using ANOVA with the Holm-Sidak test for multiple pairwise comparisons. $^{*}p< 0.05$ compared to NHEK incubated with vehicle alone.

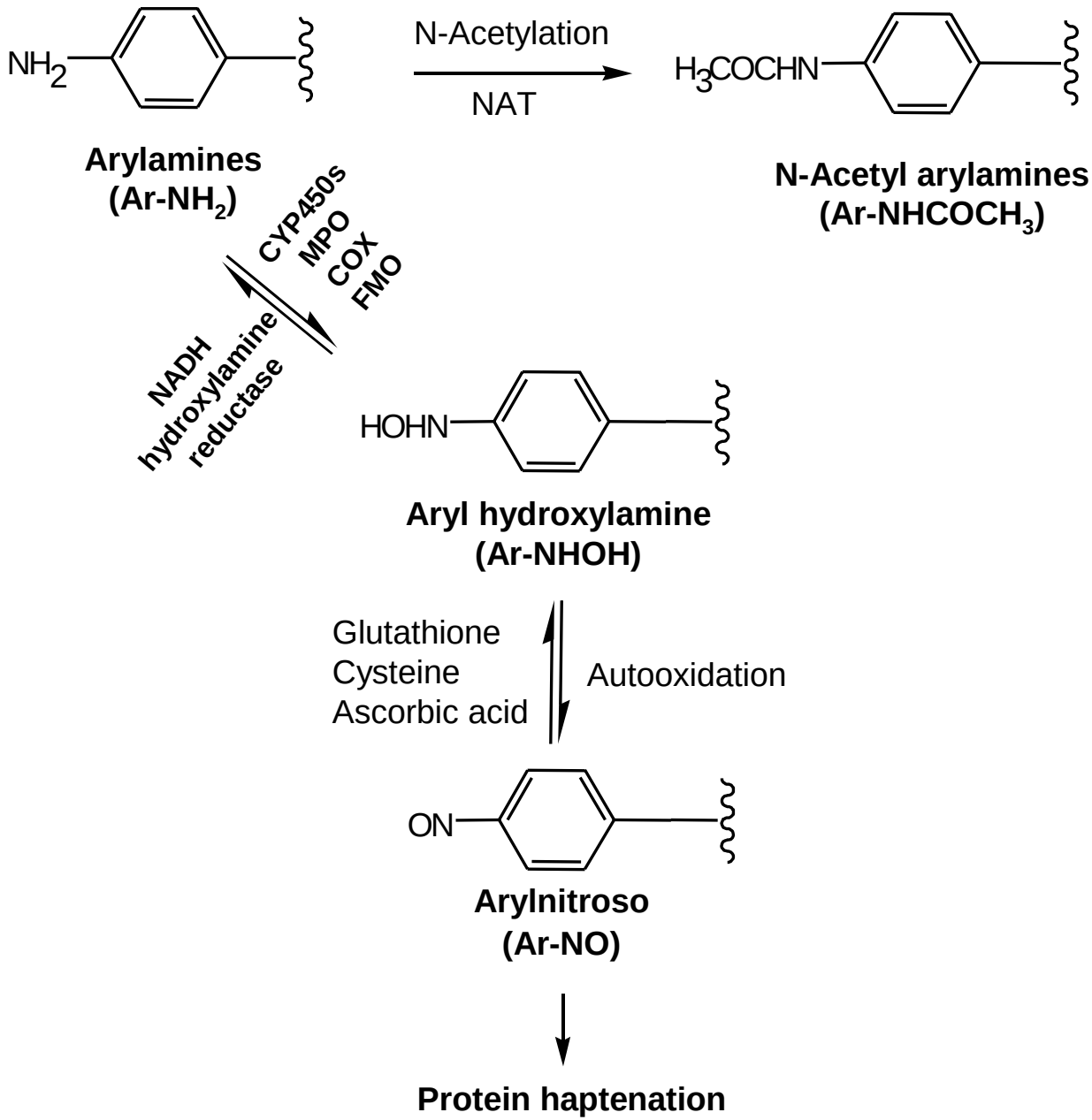

Fig.1

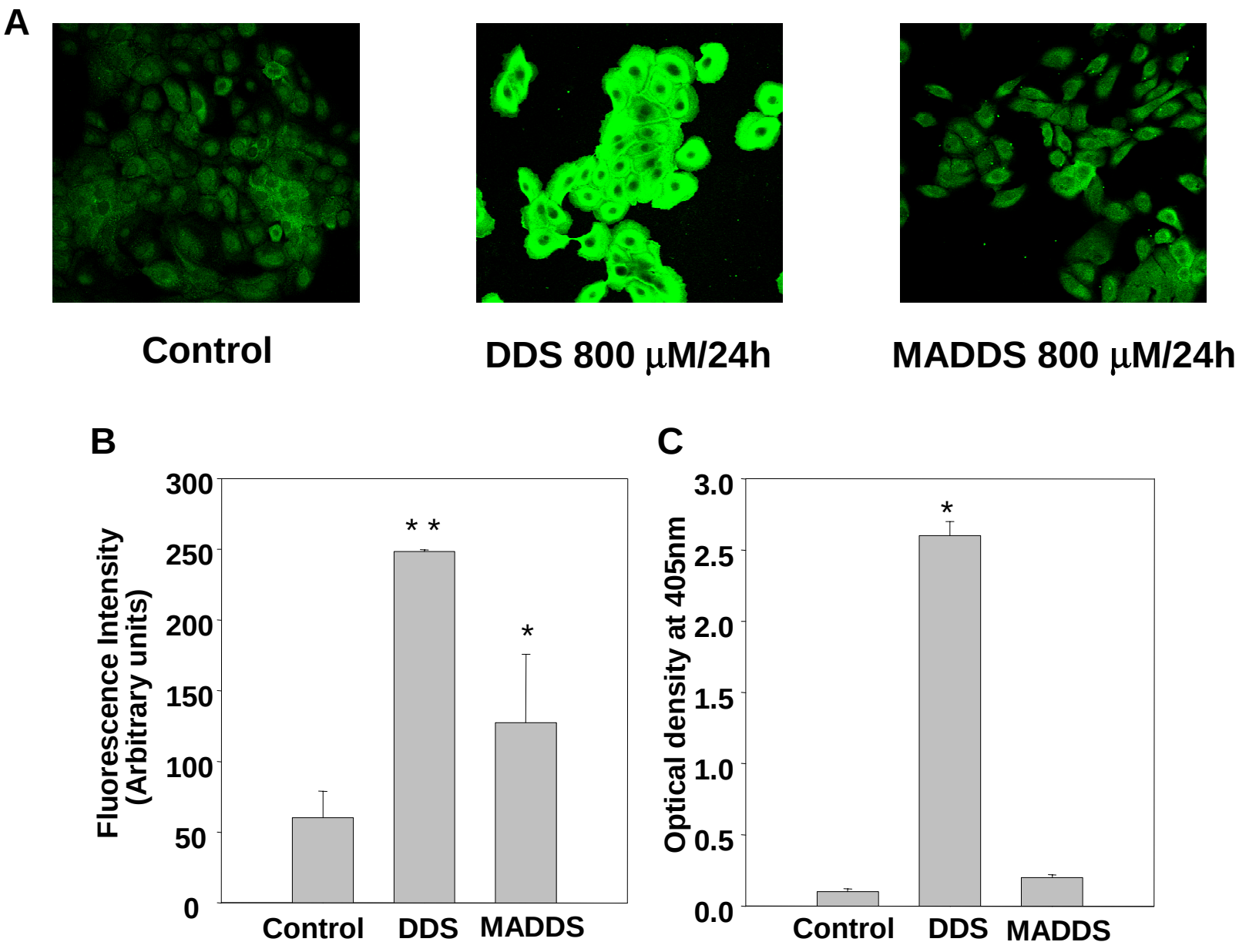

Fig.2

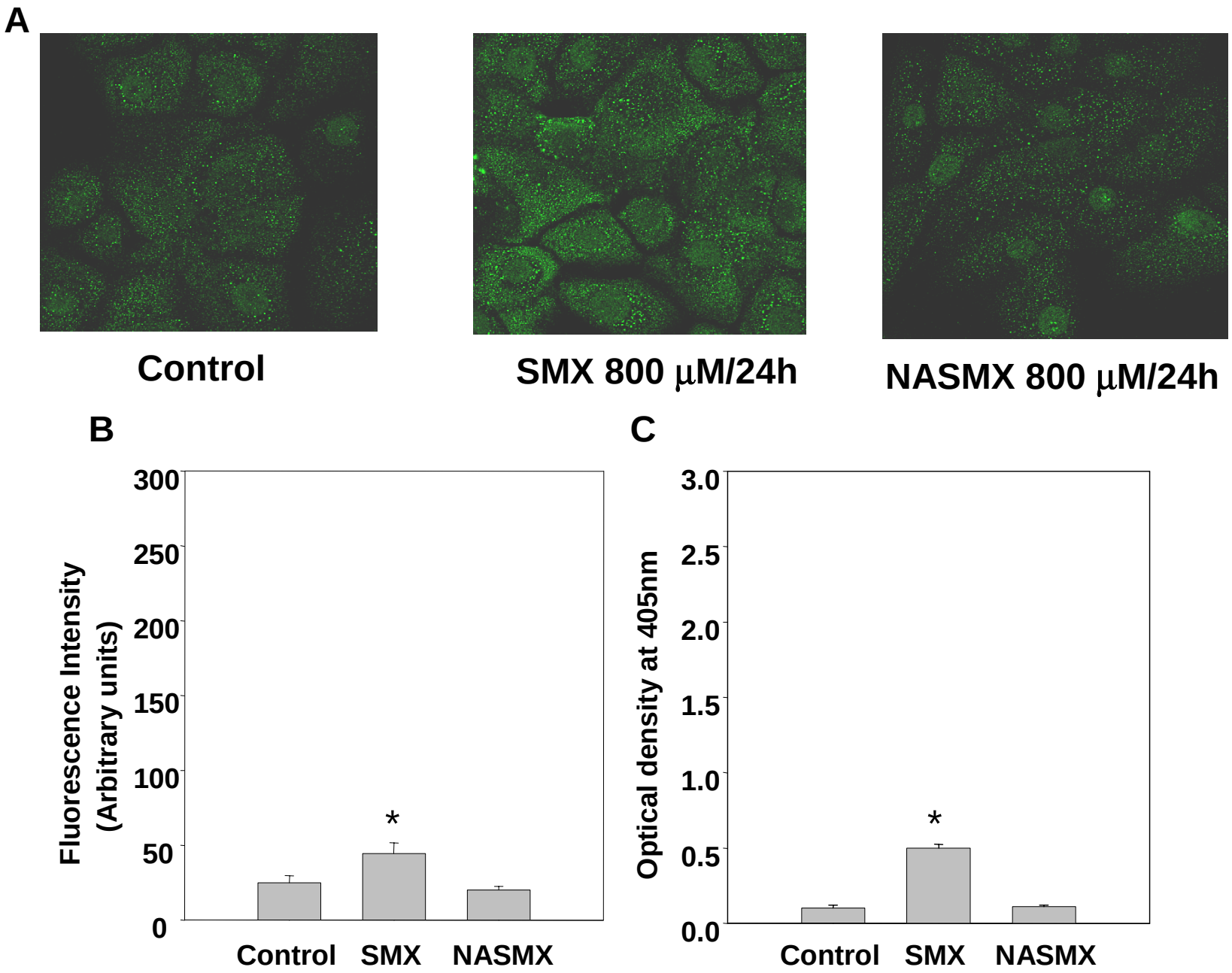

Fig.3

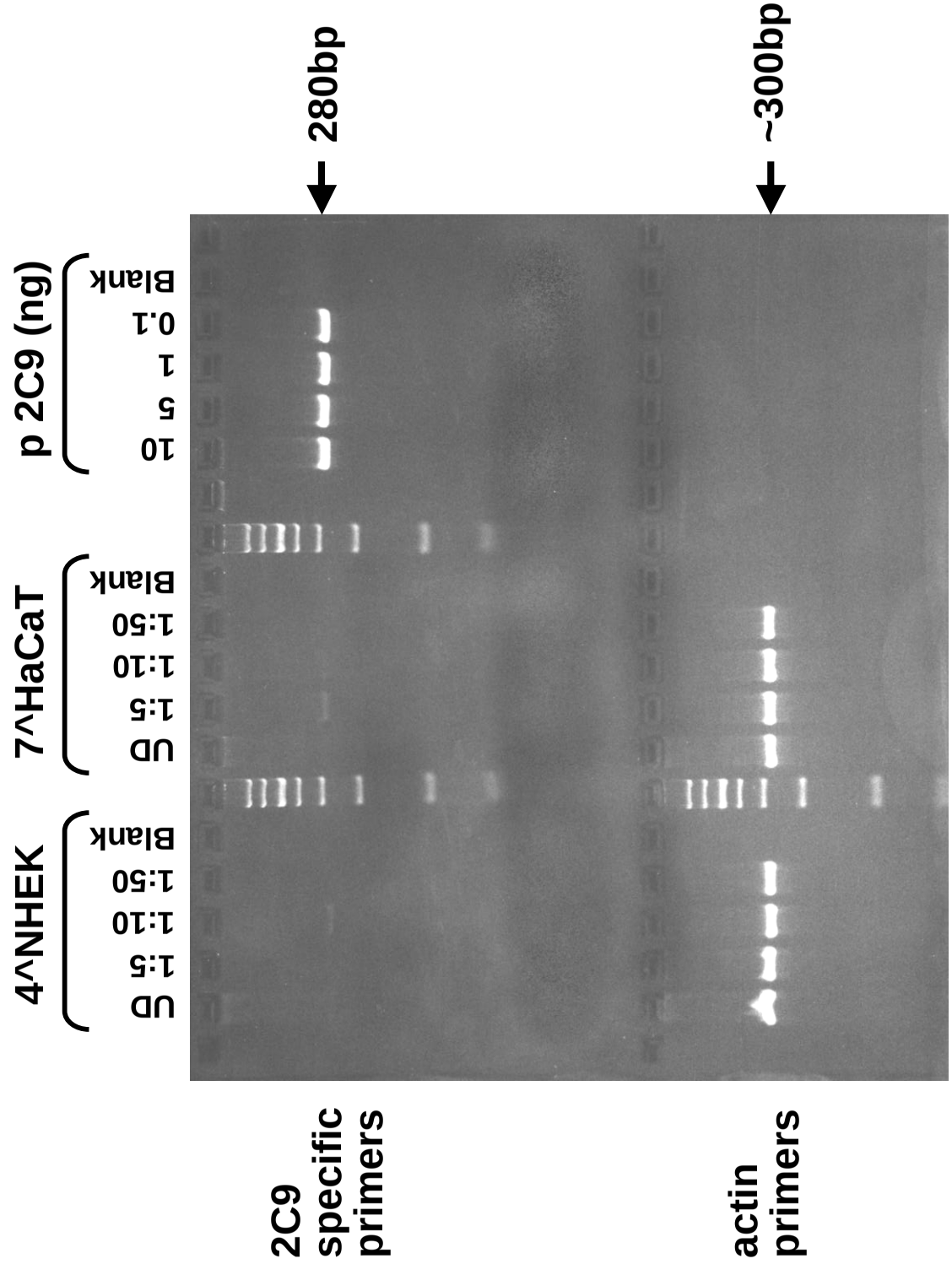

Fig.4

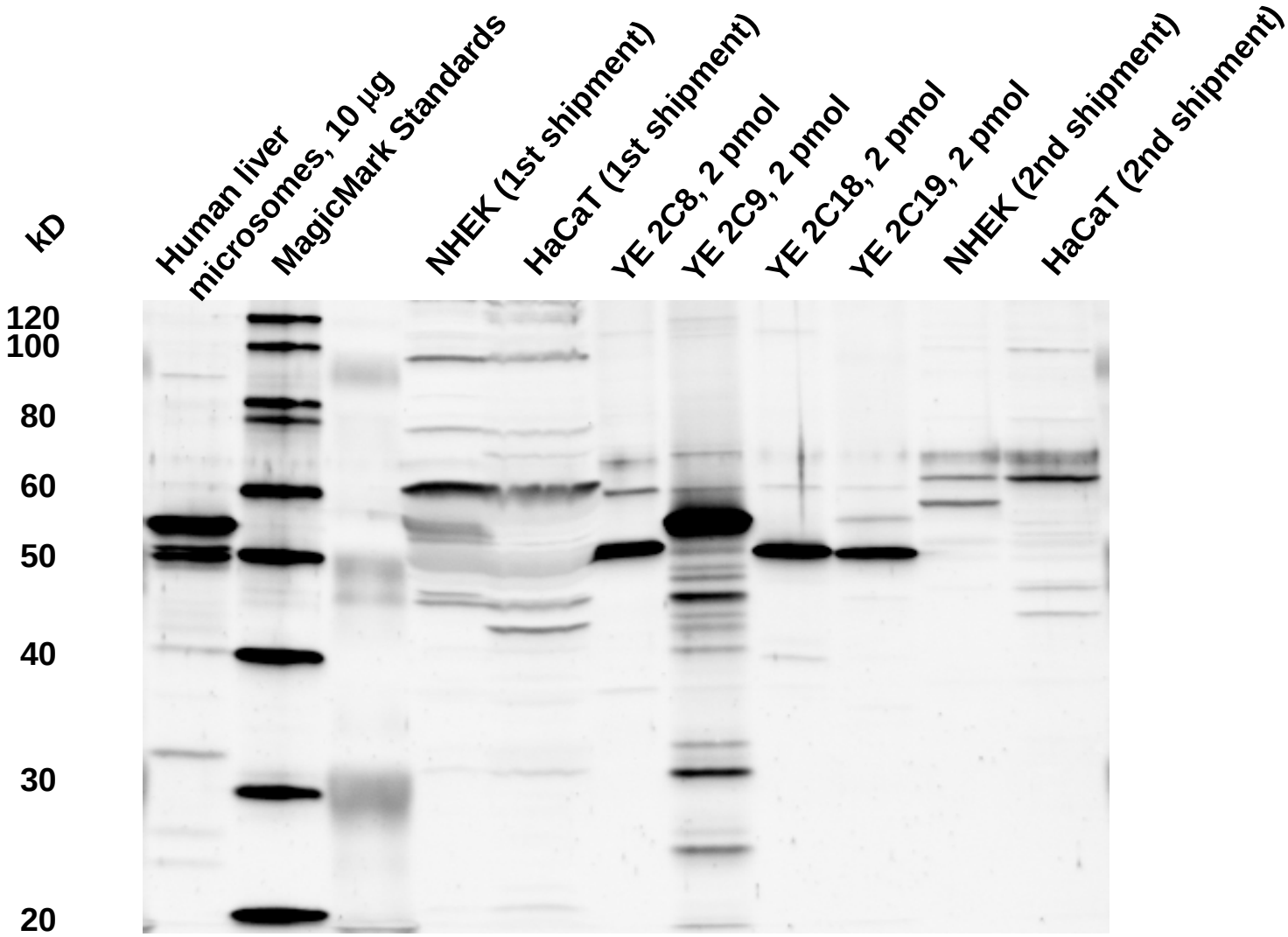

Fig.5

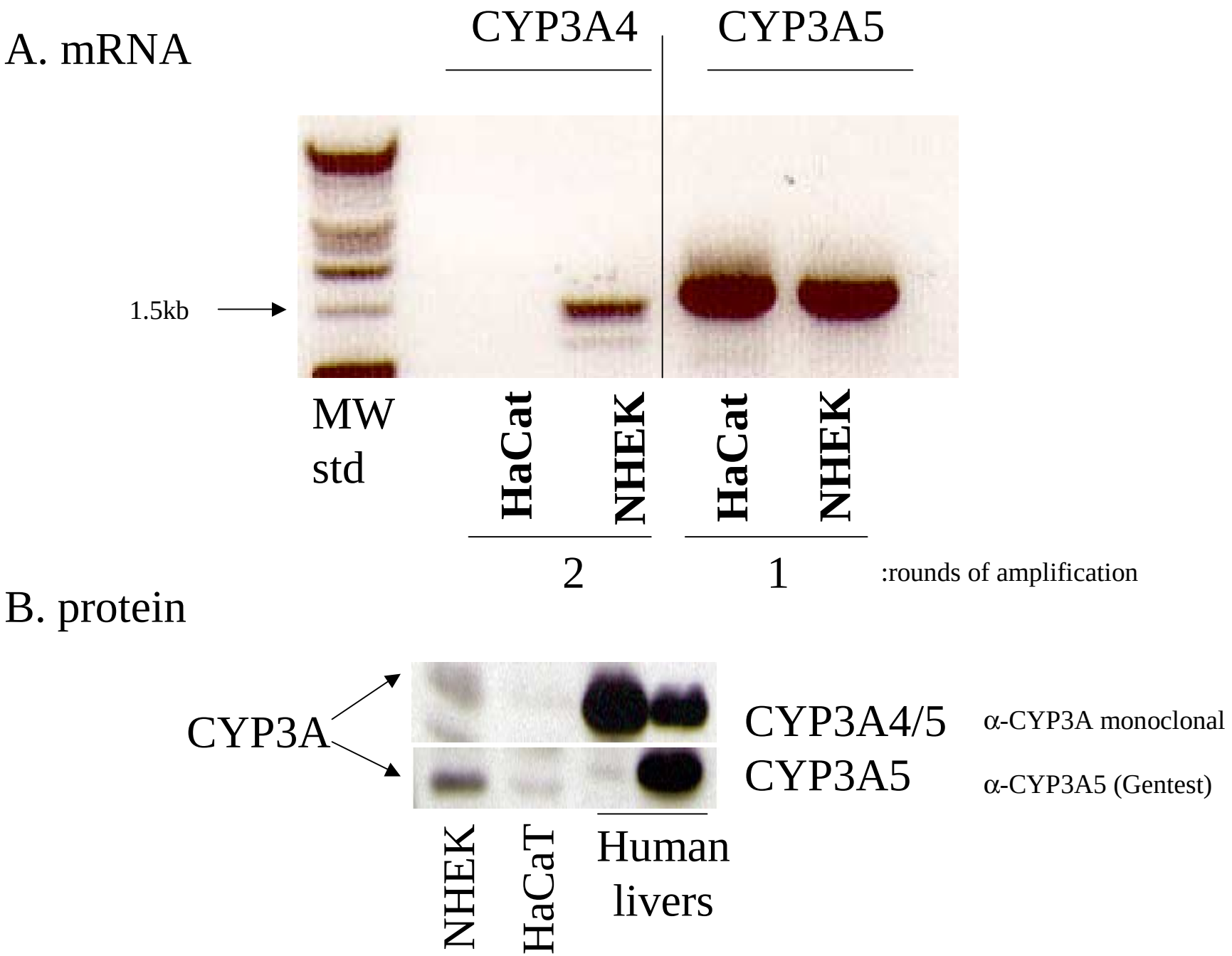

Fig.6

JPET Fast Forward. Published on July 20, 2006 as DOI: 10.1124/jpet.106.105858
This article has not been copyedited and formatted. The final version may differ from this version.

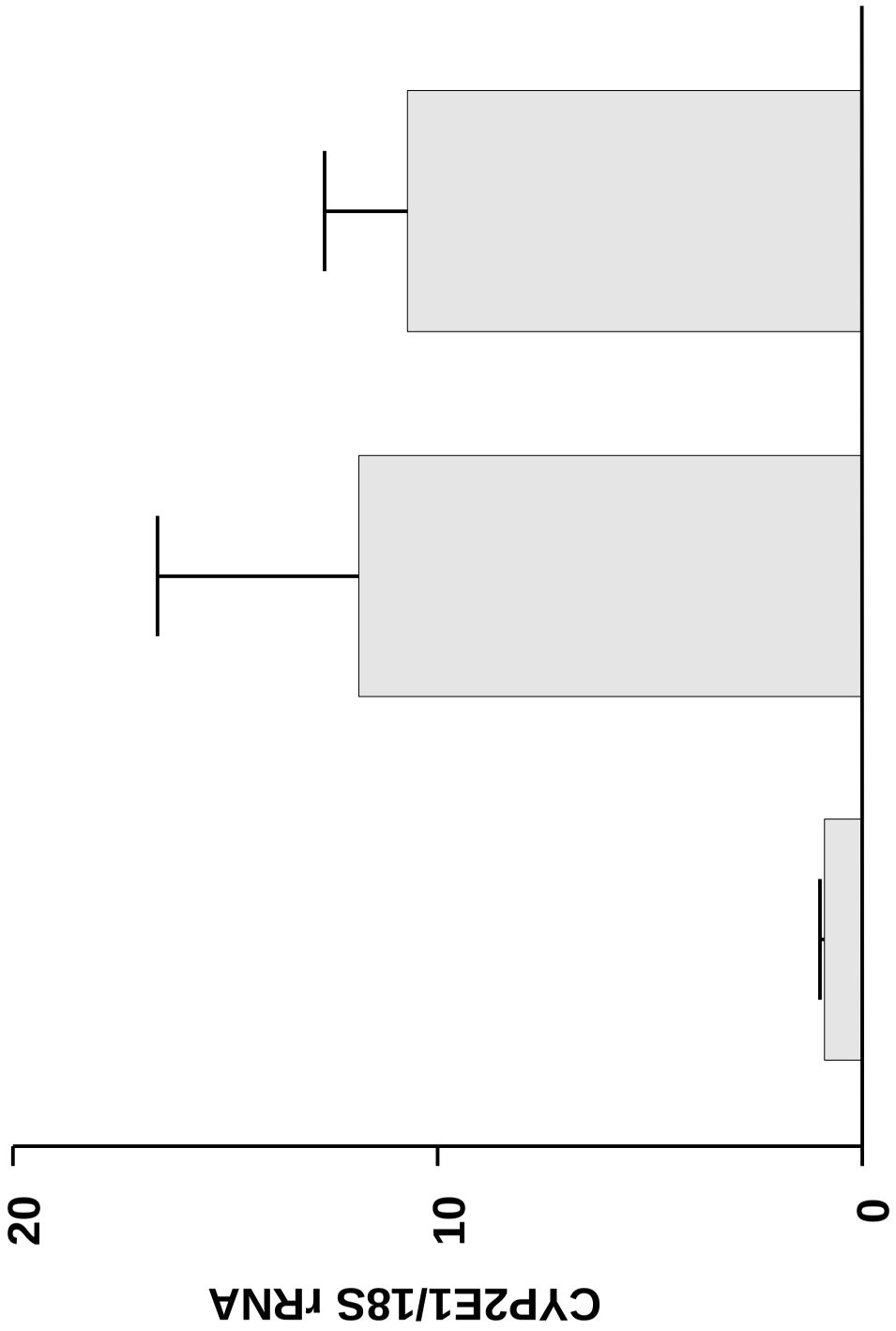

Fig.7

JPET Fast Forward. Published on July 20, 2006 as DOI: 10.1124/jpet.106.105858
This article has not been copyedited and formatted. The final version may differ from this version.

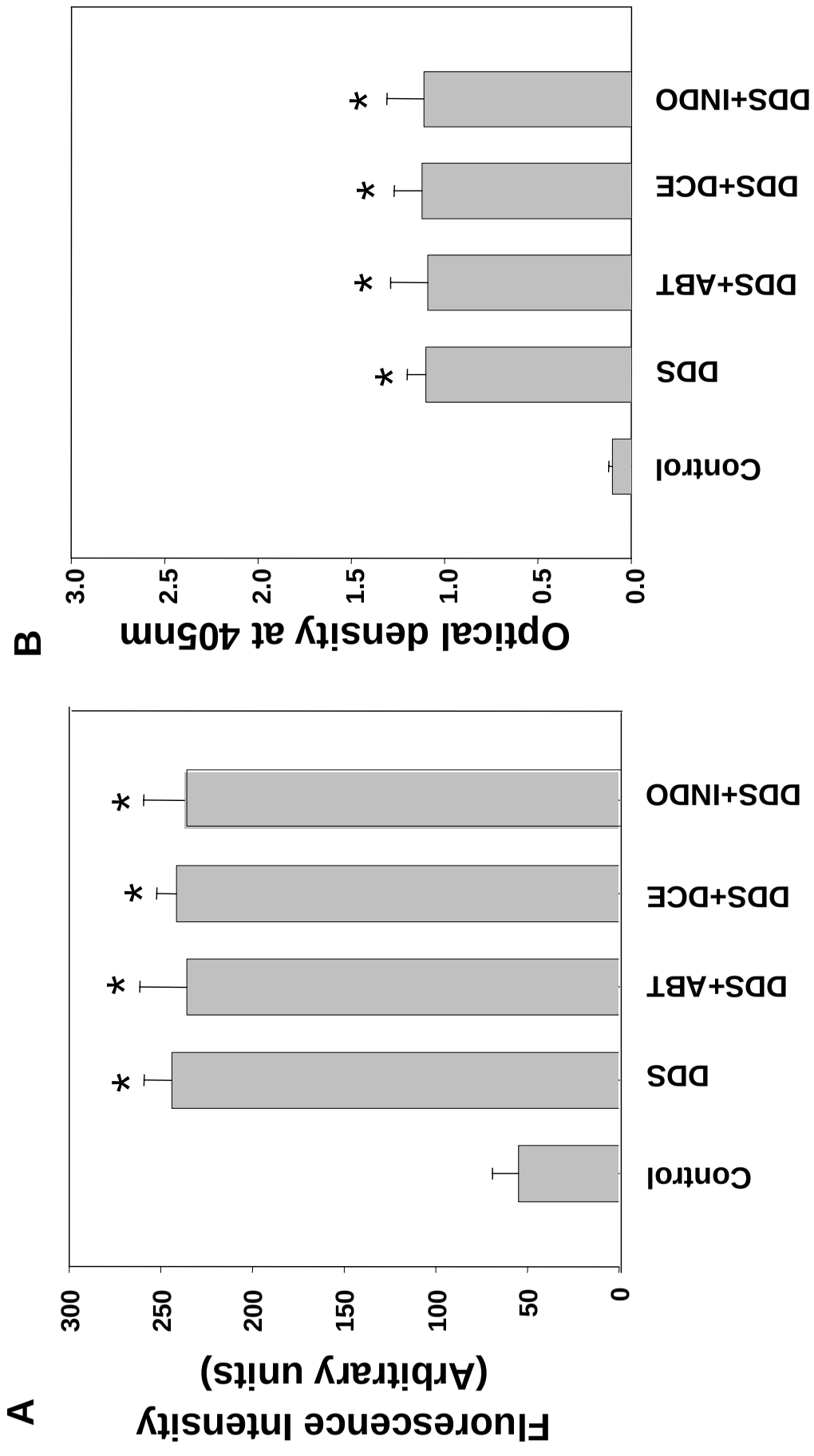

Fig.8

JPET Fast Forward. Published on July 20, 2006 as DOI: 10.1124/jpet.106.105858
This article has not been copyedited and formatted. The final version may differ from this version.

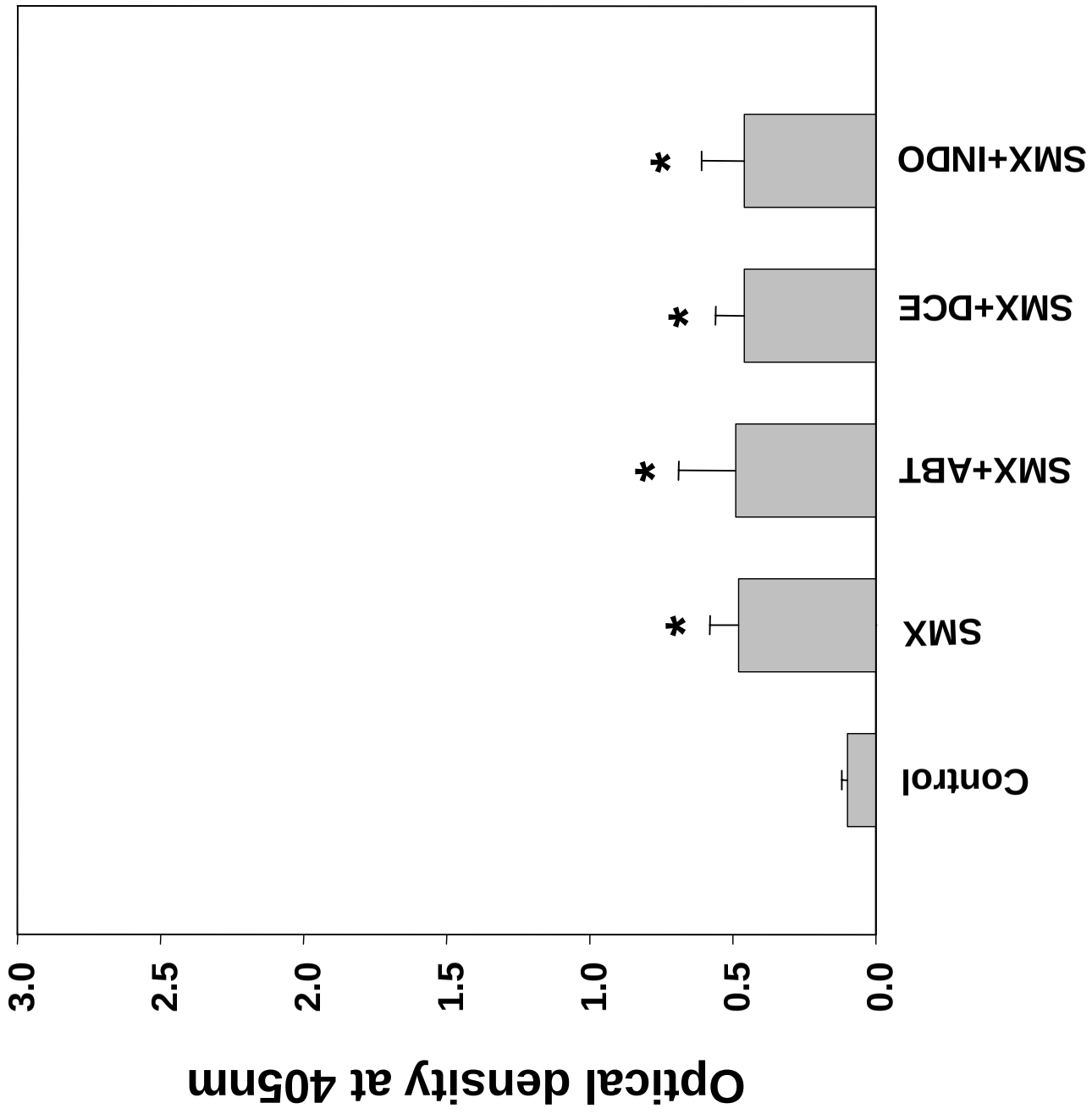

Fig.6